Journal of Translational Medicine

RESEARCH

Open Access

Targeting macrophage to myofibroblast transition by circ_0001103 for subretinal fibrosis treatment

Qi Zhang[1,2], Bing Lu[3], Lei He[4], Kai Fang[1], Xiaolong Zhu[5], Tianbing Chen[5], Yingying Zhu[1], Yinping Liu[1] and Pengfei Zhang[1*]

Abstract

Purpose Subretinal fibrosis is an important cause of visual loss in age-related macular degeneration, but its mechanism remains unclear. This study aims to investigate the role of macrophage-to-myofibroblast transition (MMT) in the formation of subretinal fibrosis and assess whether circ_0001103 can regulate the formation of subretinal fibrosis by regulating MMT.

Methods Subretinal fibrosis was induced in C57BL/6J mice by laser induction. The expression profiles of circRNAs in a choroidal neovascularization (CNV) and subretinal fibrosis mice model were accessed via microarray analysis. MMT was induced by TGF-β1 (2.5 ng/ml, 48 h). Immunohistochemistry was used to assess macrophages (F4/80), MMT (α-SMA) and fibrovascular lesions (collagenI and Isolectin B4) in vivo. The interaction between circ_0001103, miR-7240-5p, and SLC9A was assessed using a dual-luciferase reporter assay, FISH, RNA immunoprecipitation assay, qRT-PCR and western blot. Finally, immunofluorescence, paraffin section and choroidal flatmounts were used to observe the changes of MMT, subretinal fibrosis and CNV after the intervention of circ_0001103 by intravitreal injection on day 7 after laser induction in mice.

Results The results revealed that 58 circRNAs were significantly altered in the RPE-choroid-sclera complexes of CNV mice ($p < 0.05$, fold change > 2.0). Additionally, circ_0001103 increased in MMT and subretinal fibrosis mice. Circ_0001103 can sponge miR-7240-5p targeting SLC9A to modulate MMT in vitro. Inhibition of circ_0001103 can suppress MMT, subretinal fibrosis and CNV leakage.

Conclusion circ_0001103 sponge adsorption miR-7240-5p regulates SLC9A1-mediated MMT and subretinal fibrosis. Inhibition of circ_0001103 can suppress subretinal fibrosis and CNV leakage by inhibiting MMT.

Keywords Age-related macular degeneration, Subretinal fibrosis, Macrophage to myofibroblast transition, circ_0001103, miR-7240-5p

*Correspondence:
Pengfei Zhang
zhangpengfei1023@126.com
Full list of author information is available at the end of the article

Age-related macular degeneration (AMD) is the leading cause of irreversible blindness in people aged 55 [1]. It is predicted that number of new cases of early and late AMD patients in 2050 would be 39.05 million and 6.41 million, respectively [2]. Based on pathological features, AMD is divided into two types: nonneovascular AMD and neovascular AMD [3]. Neovascular AMD is mainly characterized by choroidal neovascularization (CNV), which is the main subtype that causes vision loss in AMD patients [4]. Many studies have confirmed that vascular endothelial growth factor (VEGF) is the main factor promoting the formation of CNV, so targeted VEGF is the first-line treatment method for neovascular AMD [5]. However, anti-VEGF therapy cannot prevent the progression of subretinal fibrosis [6]. Subretinal fibrosis is the main reason affecting the treatment of neovascular AMD and its visual prognosis [7]. If neovascular AMD is not treated, according to its natural course, the CNV progression to subretinal fibrosis, which leads to blindness [8]. What's more, clinical observation over a period of 2 to 6 years found that after repeated injection of anti-VEGF drugs, subretinal fibrosis and scarring occurred in about 50% of patients, resulting in severe visual impairment [9, 10]. Therefore, it is of great clinical significance to explore the key mechanism of the formation of subretinal fibrosis in the process of neovascular AMD and find effective intervention measures to improve the visual function of patients with synergistic anti-VEGF.

Subretinal fibrosis is a complex pathological process involving multiple cells [8, 11, 12], such as immune cells, myofibroblasts and excessive amounts of extracellular matrix proteins [13]. Myofibroblasts play a crucial role in the process of fibrosis formation. However, myofibroblasts is not present in the macula, which is differentiated from resident retinal cells or infiltrating inflammatory cells [11]. Studies have shown that myofibroblasts can be derived not only from pericytes, epithelial cells [14], endothelial cells [15], but can also be derived from bone marrow-derived monocytes.

Our previous studies found that macrophages were infiltrated in CNV lesions and played a key role [16, 17]. Recent studies have found that macrophage to myofibroblast transition (MMT) is involved in the formation of CNV and subretinal fibrosis, and played a key role [18]. However, it is unclear whether effective intervention in MMT is related to the formation of subretinal fibrosis.

Circular non-coding RNAs are a noval class of widely expressed non-coding RNAs. It consists of a covalently closed continuous ring, lacking a 5' cap and 3' tail. The type of RNA formed by this reverse splicing is not only relatively stable, but also more tissue-specific. Many circRNAs have been successfully demonstrated as biomarkers or therapeutic targets for many different diseases [19]. CircRNAs are involved in regulating physiological and pathological responses within cells in a variety of ways. If circRNAs are located in the cytoplasm, they can sponge adsorb downstream microRNAs or competitively bind to corresponding microRNAs, thereby regulating the expression of target genes and playing a biological role [19]. Studies have shown that the expression of cyclic RNA is abnormal in vascular diseases, neurodegenerative diseases and cancer, and in several retinal diseases, such as proliferative vitreoretinopathy and diabetes retinopathy [20–23]. However, the role of circular RNA in retinal fibrosis is still unknown.

In this study, we intend to establish a laser-induced CNV mouse model, and by sequencing the RPE-choroid-sclera complex of CNV mice, we can obtain the differential expression of circular RNA between CNV mice and normal mice. To investigate the role of circular non-coding RNA in the formation of MMT and subretinal fibrosis, and to provide some experimental basis for exploring therapeutic targets of subretinal fibrosis.

Materials and methods

Ethics statement

The animal experiments were approved by the Ethics Committee of the First Affiliated Hospital of Wannan Medical College (Yijishan hospital). All the mice was handled according to the rules of the association Vision and ophthalmology research Animal applications in ophthalmology and vision Research.

Cell culture and treatment

RAW264.7 macrophage cells were cultured with DMEM medium containing 10% fetal bovine serum. Macrophages were stimulated with TGF-β1 (2.5 ng/ml, USA, PeproTech) for 48 h. Small interfering RNAs (siRNAs) were designed and synthesized by Guangzhou RiboBio Co., Ltd. The siRNA target sequences were shown in Table 1.

Quantitative real-time PCR

Total RNA was extracted from cells/tissues using a RNA extraction kit (Qiagen, Netherlands), and RNA concentration and purity were detected using an ultraviolet spectrophotometer. cDNA synthesis: (1) removal of genomic DNA, (2) reverse transcription reaction to obtain cDNA. After synthesis, the cDNA was frozen at − 80 ℃ for future use. Primers were designed and synthesized (Table 1). qRT-PCR reaction was performed, and the standard curve was analyzed.

Western blotting

After the protein was extracted from the cells/tissues, the protein concentration was determined by BCA

Table 1 Gene sequences for qRT-PCR

Gene	Sequences
mmu_circ_0001103	Forward: 5′-CCAATCAGTCGGGCTCCTAT-3′ Reverse: 5′-GCCTTATGTGCGATCGGTTC-3′
mmu_circ_0000270	Forward: 5′-CTCATAGGCTACAGTCGGGG-3′ Reverse: 5′-TGGGGTCTTGCAGATGTCC-3′
mmu_circ_0000273	Forward: 5′-ATCAGTGGACAGCTTGTGGA-3′ Reverse: 5′-CGAACGAGGTAGACATGAGC-3′
mmu_circ_0000008	Forward: 5′-ATCCGTCCCACCAGTTCATT-3′ Reverse: 5′-GTGTGTTTGGCTCTTCTGGG-3′
mmu_circ_0000214	Forward: 5′-AGAGAACGAGAGAGACACCG-3′ Reverse: 5′-CTGCTTGAGATTGCCCGATT-3′
mmu_circ_0000894	Forward: 5′-TCACTATGAGCGGGTTGTCT-3′ Reverse: 5′-ACCAATGGCCAATGTTGCAA-3′
mmu_circ_0001670	Forward: 5′-GCTTTGGCCCTGTTAGTGTC-3′ Reverse: 5′-AGCAGATGAATAACGCCAGG-3′
mmu_circ_0008802	Forward: 5′-GGGGAAAGTGAAGCATGAAGG-3′ Reverse: 5′-CACCTTCATCTTGGCCTTCAG-3′
mmu_circ_0001393	Forward: 5′-AGCCAAAGGAGGTGATGTCC-3′ Reverse: 5′-GATGTCCTCGCTCTCAAACG-3′
mmu_circ_0000887	Forward: 5′-AGTTAGTGTCCGGGATGTGG-3′ Reverse: 5′-TTCTTATCACACAGGCCGGT-3′
mmu-SLC9A1	Forward: 5′-CATCCTTGTCTTCGGGGAGTC-3′ Reverse: 5′-GGAGGTGAAAGCTGCGATTAC-3′
mmu-α-SMA	Forward: 5′-GTCCCAGACATCAGGGAGTAA-3′ Reverse: 5′-TCGGATACTTCAGCGTCAGGA-3′
GAPDH	Forward: 5′-AAGCCCATCACCATCTTCCA-3′ Reverse: 5′-CACCAGTAGACTCCACGACA-3′
siRNA-1 (mmu_circ_0001103)	Forward: 5′-ACCCUGUGGUGCAGAAGAATT-3′ Reverse: 5′-UUCUUCUGCACCACAGGGUTT-3′
siRNA-2 (mmu_circ_0001103)	Forward: 5′-GUGCAGAAGAACCGAUCGCTT-3′ Reverse: 5′-GCGAUCGGUUCUUCUGCACTT-3′
siRNA-3 (mmu_circ_0001103)	Forward: 5′-CACCCUGUGGUGCAGAAGATT-3′ Reverse: 5′-UCUUCUGCACCACAGGGUGTT-3′
siRNA-4 (mmu_circ_0001103)	Forward: 5′-GGUGCAGAAGAACCGAUCGTT-3′ Reverse: 5′-CGAUCGGUUCUUCUGCACCTT-3′
siRNA-NC (mmu_circ_0001103)	Forward: 5′-GGGCUAAUGAACAAUAAUATT-3′ Reverse: 5′-UAUUAUUGUUCAUUAGCCCTT-3′
mmu-miR-7240-5p mimics	Forward: 5′-UUGGAGAGGACCGCCGUC GGA-3′ Reverse: 5′-CGACGGCGGUCCUCUCCAAUU-3′

method. The protein samples were transferred to SDS-PAGE gel for electrophoresis and protein separation, and then transferred to PVDF membrane. A sealing solution containing 5% buttermilk was prepared and closed for 2 h, and incubated overnight at 4℃ overtnight with primary antibody. The antibodies included α-SMA (Abcam Cat#ab7817), SLC9A (Affinity Biosciences Cat#DF9933).

Laser-induced CNV in mice and treatment

C57/BL6J male mice were taken, and after the mice were completely anesthetized, slit-lamp was used to examine the eyes of the mice. The best position is around the optic papilla at 1.5-2PD from the optic disc. Using 532 nm laser (multi-wavelength laser therapy machine, Zeiss Company, USA) photocoagulation 4–6 points, the operation can be implemented according to the wavelength of 532 nm, power of 100mW, spot diameter of 50 μm, exposure time of 100 ms standard implementation. The success criteria of laser molding: bubbles produced after photocoagulation break the Brunch membrane. Mice were administrated with adeno-associated virus vectors containing circ_0001103 small interfering RNA or scrambled shRNA by intravitreal injection on day 1 after laser induction. The eyes were enucleated for testing on day 7 after laser.

Immunohistochemistry staining

Eyeballs of each group (6 eyeballs per group) were enucleated, and serial 6-μm sections were prepared on day 7 after laser. The distance from the disrupted RPE layer to the top of the lesion was chosed for imunohistochemistry staining. For choroidal flatmounts, the eyeball was cut open, the anterior segment was removed, and the retinal nerve layer was carefully stripped to obtain the RPE-choroid-sclera complex. The tissue was spread on a slide, sealed with glycerin, and observed under confocal microscope. Incubate primary antibody included: Alexa Fluor®-594 conjugated isolectin (GS-IB4; Invitrogen, Carlsbad, CA, USA), F4/80(Abcam Cat#ab6640), college I (Abcam Cat#ab34710), α-SMA (Abcam Cat#ab7817).

Nucleo-cytoplasmic separation

The nuclear cytoplasmic separation kit (Norgen Biotek Corp, Canada) was used for nuclear cytoplasmic separation. Cytoplasmic and nuclear markers U6 and GAPDH control the effectiveness of cell isolation, respectively.

Fluorescent in situ hybridization (FISH)

The induced MMT cells were inoculated in confocal small dishes and cultured to a suitable cell density. After the cells were fixed, 0.1%TritonX was added at room temperature for 15 min to make the cells permeable. Then hybridization buffer and appropriate concentration of probe were added, hybridization overnight at 37 ℃, and excess hybridization solution and probe were fully washed. Add DAPI and stain away from light for 10–20 min. The distribution of circRNA in cells was observed by confocal microscopy. circRNA probes and RNA FISH kits are derived from the Gemma gene (GenePharma, Shanghai, China).

Luciferase reporter assay

All double luciferase experiments were performed in MTT cells. circRNA 0001103-WT/circRNA 0001103-Mut (GenePharma) and SLC9A-WT/SLC9A-Mut (GenePharma) were co-transfected with miR-7240-5p

simulated/simulated NC using pmirGLO as vector, respectively. 48 h after transfection, the cells were fully lysed and tested using the double luciferase reporter gene assay kit (GenePharma) according to the kit instructions.

RNA immunoprecipitation (RIP)

Prepare the complete RIPlysis Buffer. The cells were collected and fully lyzed to prepare immunomagnetic beads. 5ul of IgG was added to the EP tube with magnetic beads, and 2ul of Ago2 (Abcam) was added to the other tube, and incubated at room temperature for 30 min. Prepare the RIP Immunoprecipitation Buffer. Move the 10ulRIPlysate supernatant into the new EP, label it as Input, incubate the EP tube, and rotate 4 ℃ overnight. Prepare proteinase K buffer, melt the EP tube labeled Input, add 107 μl RIP Wash buffer, 15 μl 10% SDS18 μl 10 mg/ml proteinase K, and make the final volume 150 μl. Incubate all EP tubes at 55 ℃ for 30 min; Rapid centrifugal EP tube, placed in magnetic plus. Transfer the supernatant to the new EP tube and add 250 μl RIP Wash buffer to make the tube volume reach 400ul. 850 μl of anhydrous ethanol, stored at −80 ℃ overnight. RNA-Binding Protein Immunoprecipitation Kit is Magna RIP Kit (Catalog No. 17-700).

RNase R

The extracted RNA was divided into two tubes of the same volume. According to the Reaction system provided by the instruction manual of Ribonuclease R kit (Giesay, Guangdong, China), appropriate amount of RNase R, 10X Reaction Buffer and RNASe-free Watersh were added to one tube. The two tubes of RNA were then subjected to RT-RNA analysis.

Statistical analysis

Graph Pad Prism (V6, GraphPad Software, San Diego, USA) was used to conduct statistical analysis. All data were expressed as means ± SEM. For normally distributed data, statistical analysis was performed using 2-tailed Student's t test or one-way analysis of variance (ANOVA). $^{*}p < 0.05$ was considered statistically significant.

Results

CircRNA expression profiles in lase induced CNV mouse model

Firstly, we established a laser-induced mouse model of CNV and subretinal fibrosis. Then, using a profiling microarray, we identified 58 circRNAs (32 upregulated, 26 downregulated) were significantly differentially on day 7 after laser induction (Fold change > 2.0, $p < 0.01$, Fig. 1A). The significantly differentially expressed circRNAs are presented as scatter plots (Fig. 1B). To verify the microarray data results, twelve dysregulated circRNAs (six highly expressed circRNAs and six lowly expressed circRNAs) were randomly selected for qRT-PCR analysis (Fig. 1C). The microarray and qRT-PCR expression trends were very similar. The results showed that the reliability and reproducibility of these circRNA expression profiles were verified.

circ_0001103 expression is up-regulated in macrophage-to-myofibroblast transition and in laser-induced CNV lesions

It has been found that TGF-β1 was highly expressed in the CNV microenvironment [18]. In this study, we stimulated raw264.7 macrophages using TGF-β1 at 2.5 ng/ml for 48 h (USA, PeproTech), and finally induced macrophage to myofibroblast transition. We detected α-SMA, a marker of MMT, and found that α-SMA expression were significantly increased at both mRNA and protein levels ($p < 0.001$, Fig. 2A–C), circ_0001103 expression was also increased in MMT ($p < 0.001$, Fig. 2D). It is known that the function of circRNA is related to its localization in cells, we used FISH to show that circ_0001103 was mainly expressed in the cytoplasm of MMT (Fig. 2E). We then estimated circ_0001103 stability by treating the total RNAs from MMT with RNase R. The results showed circ_0001103 was resistant to RNase R digestion, while linear mRNA 0001103 was easily degraded (Fig. 2F, G). The results suggested that circ_0001103 has good stability.

Next, we took RPE-choroid-sclera complexes of mice after laser induction on days 7, 14 and 28 to test the top 10 circRNAs of the microarray data results (Fig. S1). qRT-PCR showed that the expression of circ_0001103 (chr2:168392638-168397133) was significantly higher than that of normal tissues on days 7, 14 and 28 after laser induction ($p < 0.001$, Fig. S1).

circ_0001103 regulates macrophage-to-myofibroblast transition in vivo and in vitro

We designed four different siRNAs for circ_0001103 silencing. It was found that siRNA2 transfection could significantly reduce circ_0001103 ($p < 0.001$, Fig. 3A). Therefore, we chose siRNA2 for the experiment to detect macrophage to myofibroblast transition after induced by TGF-β1 in vitro. After circ_0001103 was decreased, α-SMA expression were significantly increased at both mRNA and protein levels ($p < 0.001$, Fig. 3B–D).

Next, we investigated the effect of circ_0001103 on macrophage to myofibroblast transition in vivo. Adeno-associated viral shRNA was intravitreally

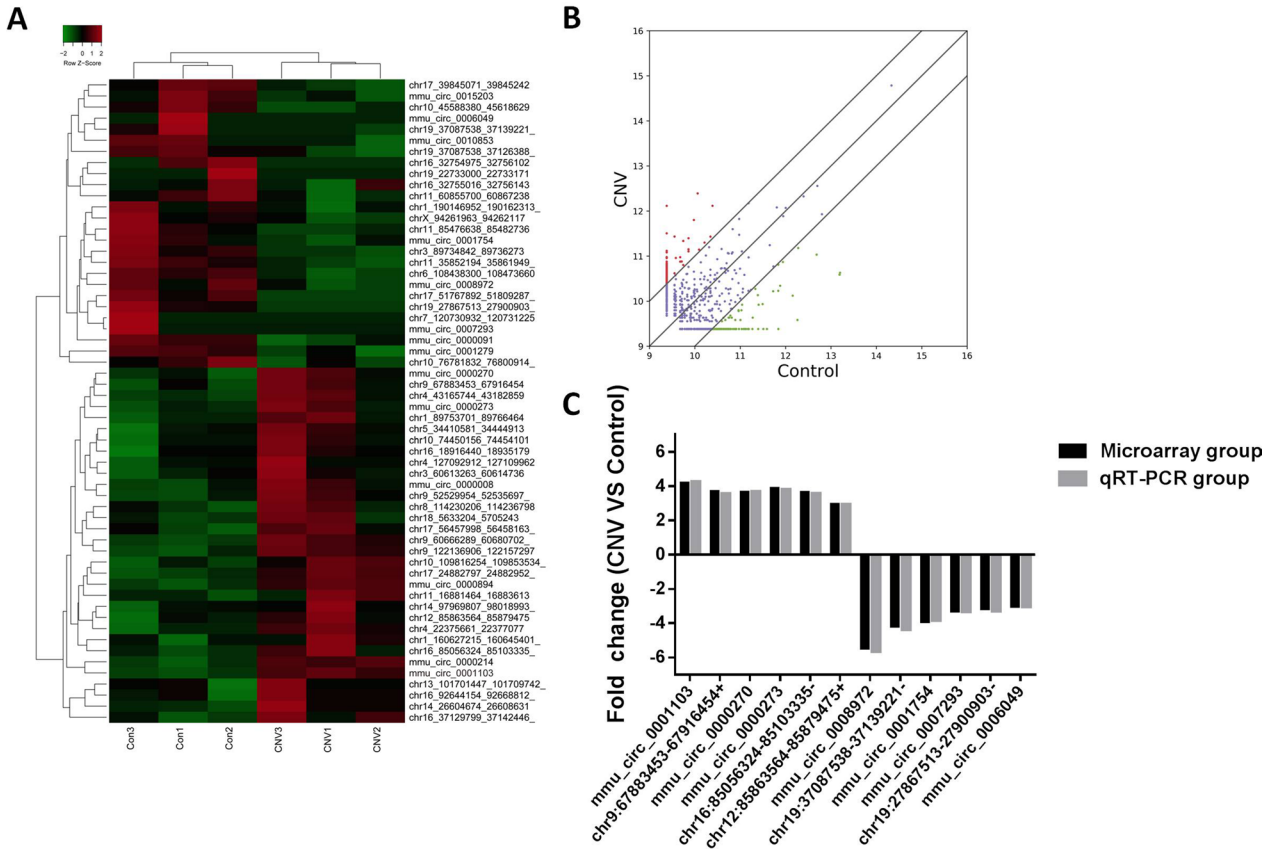

Fig. 1 CircRNA Expression Profiles in the CNV Mouse Model. Heat map (**A**) and scatter plots analysis (**B**) of differentially expressed circRNAs between CNV and control samples ($P < 0.01$, fold change > 2.0). In heat map analysis, red and blue columns refer to high and low relative expression, respectively. In plots analysis analysis, green dots indicate no change, blue and red dots indicate significantly downregulated and upregulated lncRNAs volcano plots analysis. The randomly selected 12 dysregulated circRNAs (six upregulated circRNAs and six downregulated circRNAs) for qRT-PCR analysis in (**C**). The microarray and qRT-PCR expression trends were very similar

injected on day 1 after laser photocoagulation to decreased circ_0001103 expression (Fig. 4A). At first, we examined the F4/80$^+$ macrophage infiltration and α-SMA$^+$ MMT transformation in the laser lesion area of mice on day 7 after laser. The distance from the disrupted RPE layer to the top of the lesion was chose for staining. Figure 4C zoomed in area shown in white circle in 4B. The white arrows indicate the location of F4/80 and α-SMA cells. The section results showed F4/80$^+$ cells co-express α-SMA in control group on day 7 after laser induction (Fig. 4B). Further, we chose choroidal flatmounts. The results showed F4/80 and α-SMA are co-localisation in choroidal flatmounts (Fig. 4D Ctrl group). Immunofluorescent staining showed that silences of circ_0001103 could significantly inhibit the expression of α-SMA, but could not inhibit the expression of F4/80, suggesting that inhibiting circ_0001103 could affect MMT transformation in vivo, but not macrophage on day 7 (Fig. 4D–F).

circ_0001103 regulates macrophage-to-myofibroblast transition serving as a miRNA sponge

We have found that circ_0001103 was more abundant in the cytoplasm than in the nucleus. Therefore, we speculated that circ_0001103 might act as a miRNA sponge to regulate gene expression. Circular RNA Interactome database and analysis showed that there were two potential binding sites for miR-7240-5p in circ_0001103 (Fig. 5A). We employed RNA immunoprecipitation (RIP) assays to show that Ago2 protein can enrich circ_0001103 and miR-7240-5p (Fig. 5B, C). RNA-FISH confirmed the co-localization between circ_0001103 and miR-7240-5p, which both circ_0001103 and miR-7240-5p were mainly localized in the cytoplasm of MMT (Fig. 5D).

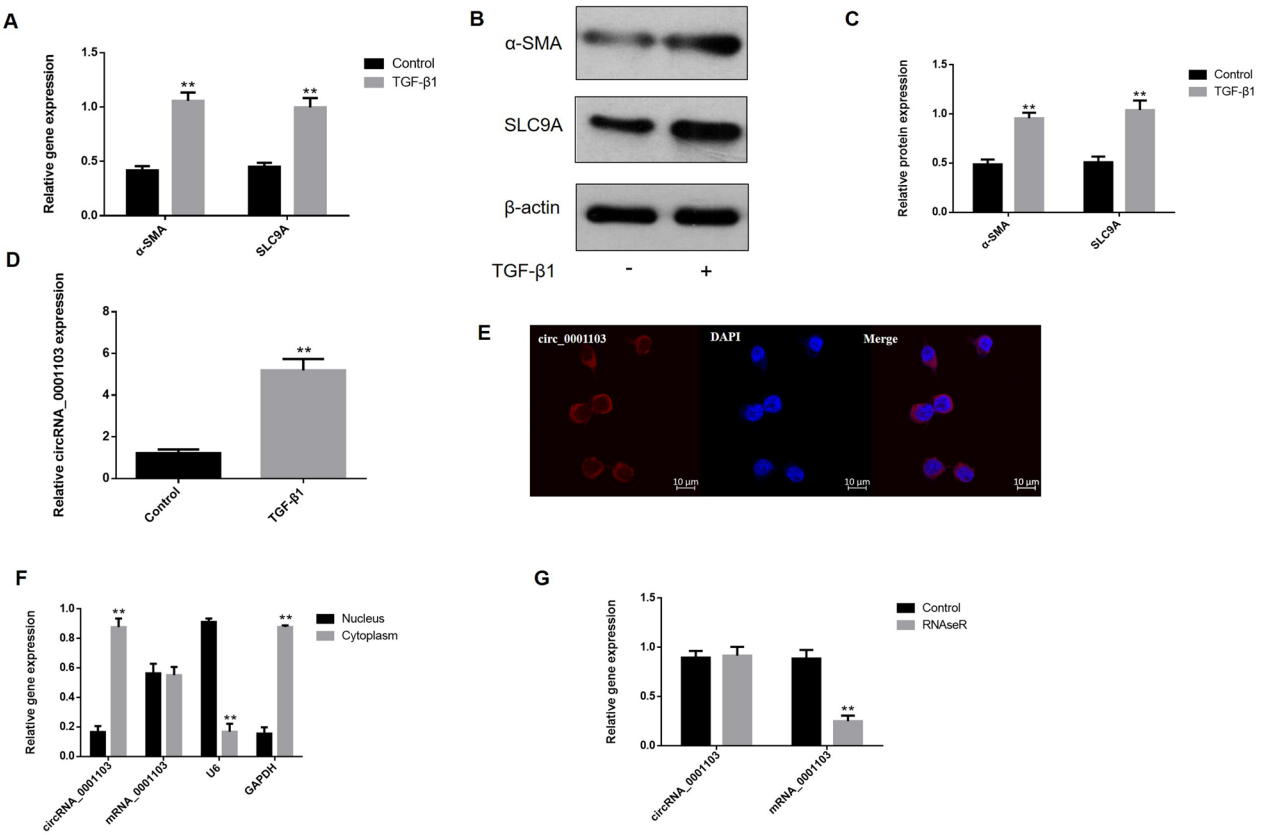

Fig. 2 circ_0001103 expression is up-regulated in macrophage-to-myofibroblast transition. Gene and protein expression of α-SMA and SLC9A (**A**–**C**) of raw264.7 macrophages stimulated by TGF-β1 (2.5 ng/ml for 48 h) in vitro increased than untreated (control). Gene expression of circRNA_0001103 (**D**) of raw264.7 macrophages stimulated by TGF-β1 (2.5 ng/ml for 48 h) also increased than untreated (control). RNA FISH was performed to detect circRNA_0001103 in raw264.7 macrophages by probes (circRNA_0001103). Nuclei were stained with 4, 6-diamidino-2-phenylindole (DAPI). circRNA_0001103 was detected mainly in the cytoplasm (**E**). Nuclei, blue; circRNA_0001103, red. Scale bar, 10 μm. The expression of circRNA_0001103, mRNA_0001103, nuclear control transcript (U6), and cytoplasm control transcript (GAPDH) were detected by qRT-PCR in the nuclei and cytoplasm of raw264.7 macrophages (**F**). qRT-PCR was conducted to detect circRNA_0001103. mRNA_0001103 was detected as the RNase R-sensitive control (**G**). Data are presented as mean + SEM, n = 6 for each time point. **p < 0.001

Next, we constructed wild type and mutant plasmids of circ_0001103. The wild type and mutant plasmid of circ_0001103 and the overexpressed gene sequence of miR-7240-5p were co-transfected into MMT to detect the fluorescence value. By the same method, wild-type and mutant SLC9A plasmid and overexpressed gene sequence of miR-7240-5p were co-transfected into MMT to detect fluorescence values. The results showed that the luciferase signal of the co-transfected group with the wild type of circ_0001103 and the over-expressed gene of miR-7240-5p decreased (Fig. 5E), indicating that circ_0001103 could sponge adsorb miR-7240-5p. In the co-transfection group of SLC9A wild-type and miR-7240-5p overexpressed genes, the luciferase signal decreased, indicating that miR-7240-5p could target gene SLC9A (Fig. 5F).

circ_0001103/miR-7240-5p/SLC9A mediates macrophage-to-myofibroblast transition in vitro

To investigate whether circ_0001103 sponging miR-7240-5p regulating SLC9A can modulate macrophage-to-myofibroblast transition, circ_0001103 was silenced by siRNA2 transfecting in MMT. Data showed that, after inhibiting circ_0001103, the gene and protein expressions of α-SMA and SLC9A decreased than TGF-β1group (Fig. 3B–D, all $p < 0.001$). Next, we transfected macrophages with miRNA-7240-5p mimic. The results showed the gene and protein expressions of α-SMA and SLC9A decreased than TGF-β1group (Fig. 3B–D, all $p < 0.001$). Then, we co-transfected macrophages with the circ_0001103 siRNA2 and miRNA-7240-5p mimic. The results showed the gene and protein expressions of α-SMA and SLC9A were significantly lower than that of TGF-β1group, circ_0001103 siRNA2 group, and miRNA-7240-5p mimic group (Fig. 3B–D, all $p < 0.001$).

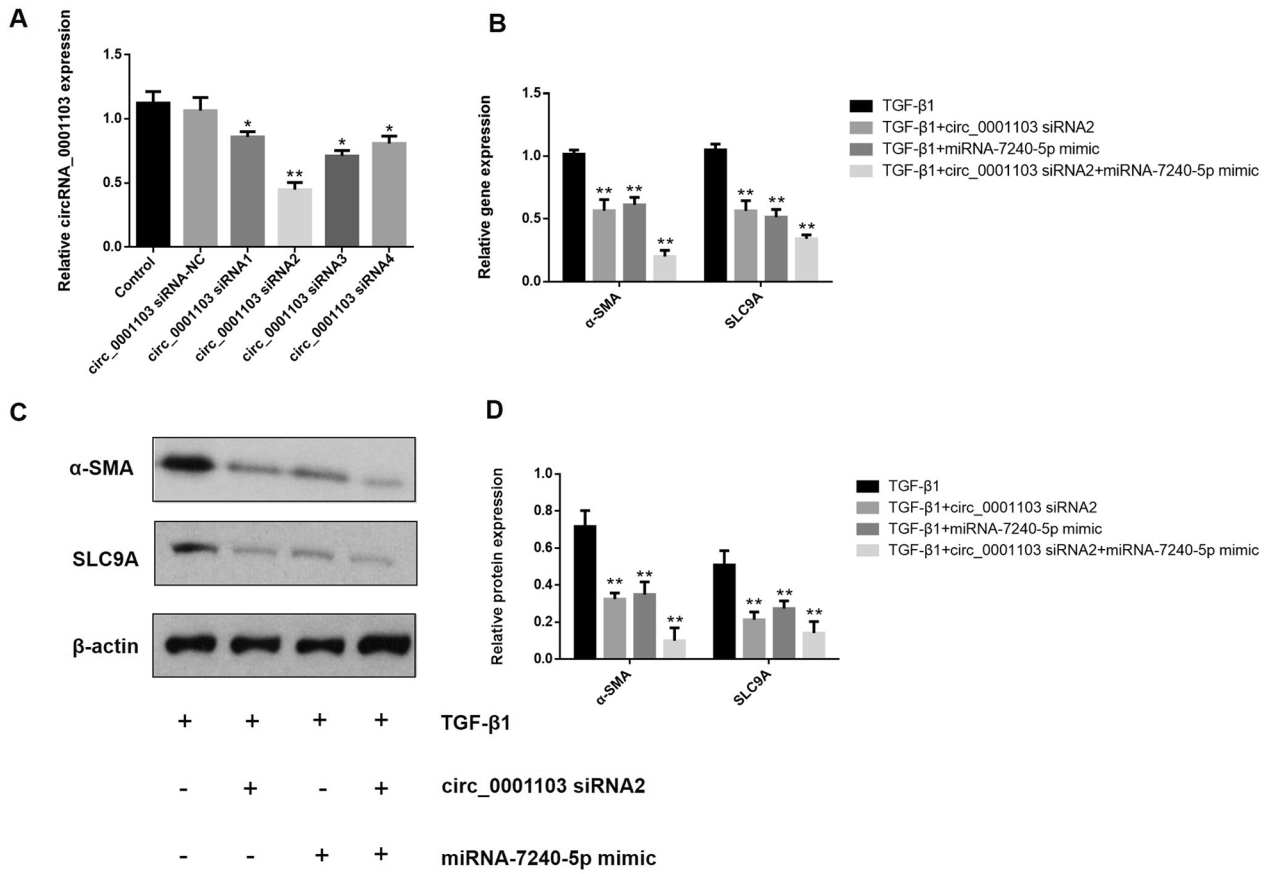

Fig. 3 circRNA_0001103/miR-7240-5p through SLC9A mediates macrophage-to-myofibroblast transition in vitro. Raw264.7 macrophages were transfected with siRNA targeting the sequence of circRNA_0001103 (4 different siRNAs for circ_0001103 silencing is designed), scrambled siRNA (siRNA-NC), or left untreated (Ctrl) for 36 h of incubation. circRNA_0001103 was significantly reduced after siRNA2 transfection ($p < 0.01$, **A**). After induced by TGF-β1, raw264.7 macrophages were transfected with circRNA_0001103 siRNA2, miR-7240-5p mimic, circRNA_0001103 siRNA2 plus miR-7240-5p mimic. Gene and protein expressions of α-SMA and SLC9A significantly decreased in circRNA_0001103 siRNA2 transfection group and miR-7240-5p mimic transfection group than TGF-β1 group (**B**–**D**, all $p < 0.001$). After co-transfected with circ_0001103 siRNA2 and miRNA-7240-5p mimic, gene and protein expressions of α-SMA and SLC9A significantly decreased than that of TGF-β1group, circ_0001103 siRNA2 group, and miRNA-7240-5p mimic group (**B**–**D**, all $p < 0.001$)

Therefore, the results indicate that circ_0001103 sponging adsorb miR-7240-5p regulates SLC9A1-mediated macrophage-to-myofibroblast transition induced by TGF-β1.

circ_0001103 regulates subretinal fibrosis and CNV in vivo

To verify the effect of circ_0001103 on CNV and subretinal fibrosis, adeno-associated viral shRNA is designed for circ_0001103 silencing, circ_0001103 shRNA was intravitreally injected at day 1 after laser photocoagulation. Immunofluorescent staining The CNV formation area was investigated by showed IB4 fluorescence staining, and the subretinal fibrosis formation area was investigated by CollegeIfluorescence staining. The results showed that silences of circ_0001103 could significantly inhibit CNV area on day 7 (Fig. 6, all $p < 0.001$), the and fibrosis area of circ_0001103 silence group were significantly reduced (Fig. 6, all $p < 0.001$). It was demonstrated that inhibition of circ_0001103 can affect the formation of CNV and subretinal fibrosis.

Discussion

In this study, through the establishment of laser-induced mouse CNV model and TGF-β1 induced MMT cell model, it is found that circ_0001103 is a key factor regulating the transformation of macrophages into myofibroblasts and inducing the formation of subretinal fibrosis. Further studies showed that circ_0001103 regulated SLC9A1-mediated macrophage transformation into myofibroblasts and the formation mechanism

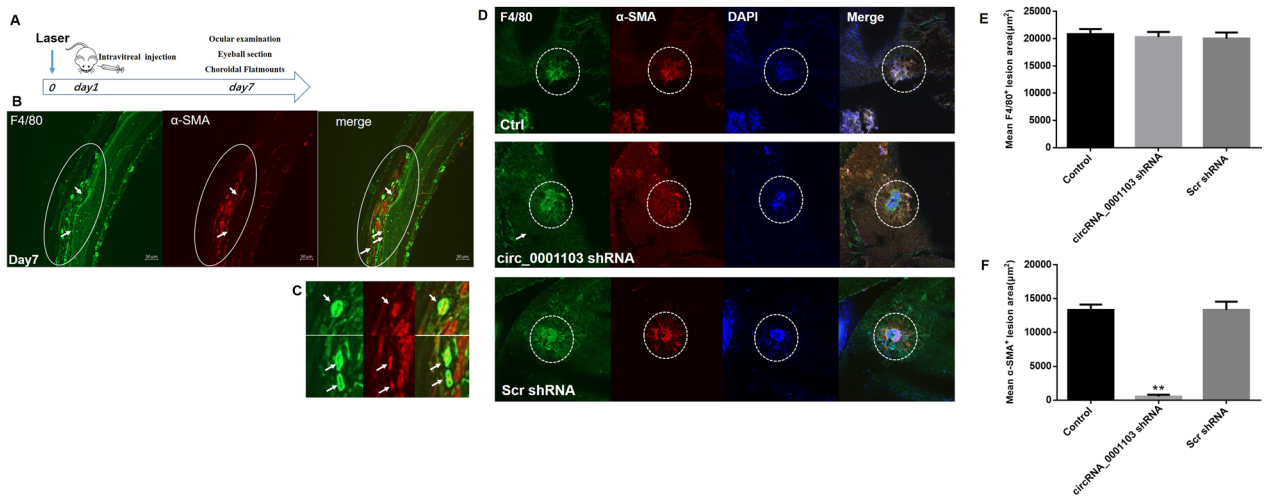

Fig. 4 F4/80$^+$α-SMA$^+$ lesions in CNV fibrotic lesions and the effect of blocking circRNA_0001103. Mice were administrated with adeno-associated virus vectors containing circRNA_0001103 small interfering RNA or scrambled shRNA by intravitreal injection on day 1 after laser induction. The eyes were enucleated for testing on day 7 after laser (**A**). Wax-embedded sections from mice laser model on day 7 after laser were stained for F4/80 (green) and α-SMA (red) and imaged by confocal microscopy. Scale bar = 50 μm. **C** zoomed in area shown in white circle in 4B. Arrows indicating F4/80 and αSMA cells. Quantitative measurement of F4/80$^+$ and α-SMA$^+$ lesions in different groups in 4D. The section results showed approximately 75% of F4/80$^+$ cells co-express α-SMA in control group on day 7 after laser induction (**B**). Choroidal flatmounts were taken on day 7 after laser treatment to stained for F4/80 (green) and α-SMA (red). The results showed F4/80 and α-SMA are co-localisation in choroidal flatmounts and approximately 75% of F4/80$^+$ cells co-express α-SMA in control group on day 7 after laser induction (**D** Ctrl group). The α-SMA$^+$ cell lesions, but not F4/80$^+$ cell lesions area receiving circRNA_0001103 small interfering RNA significantly reduced on day 7 (**D**–**F**). Data are presented as mean + SEM, n = 6 for each time point. **p < 0.001

of subretinal fibrosis through adsorption of mmu-miR-7240-5p (Fig. 7). Circ_0001103 can regulate the transformation of macrophages into myofibroblasts and the formation of subretinal fibrosis.

Subretinal fibrosis secondary to CNV is the main cause of vision loss in nAMD [24]. Formation of subretinal fibrosis is a pathological process of excessive extracellular matrix secreted by glial cells, macrophage, RPE cells, endothelial cells, and et al. [11, 25]. However, its specific pathogenesis and interventions are still unclear. Myofibroblasts are the main cells that cause subretinal fibrosis [8]. Myofibroblasts are the activated form of fibroblasts, which are thought to be differentiated from resident retinal cells or blood-derived inflammatory cells. Several studies have found that RPE cells can transform into EMT, leading to subretinal fibrosis [7, 26]. Endothelial cells through endothelial to mesenchymal transition (EndoMT) can lead to macular fibrosis [27]. In our study, it has been found that macrophages can transform into myofibroblasts in a certain microenvironment, leading to fibrosis.

Previously, we established a mouse model of laser-induced CNV formation and found that macrophages migrated to the lesion during CNV formation, Arg-1 + YM-1 + M2 macrophages can promote CNV [17, 28]. In different microenvironments, macrophages can differentiate into different subtypes, and different subtypes of macrophages in turn play different roles in shaping the environment [29, 30]. In this study, we have found that MMT marker α-SMA can be co-expressed

(See figure on next page.)

Fig. 5 circ_0001103 sponge adsorption miR-7240-5p regulates SLC9A1-mediated macrophage-to-myofibroblast transition. The potential binding sites sequence of miR-7240-5p on circRNA_0001103, SLC9A on miR-7240-5p (**A**). The cytoplasm and total cellular fractions were isolated from MTT cells, and then immunoprecipitated using IgG or Ago2 antibody. circRNA_0001103 and miR-7240-5p amount in the immunoprecipitate was determined by qRT-PCR (**B**, **C**, all $p < 0.001$). RNA-FISH were conducted to detect circRNA_0001103 and miR-7240-5p expression in circRNA_0001103 and miR-7240-5p. The results showed that both circRNA_0001103 and miR-7240-5p mostly existed in the cytoplasm (**D**). Scale bar, 20 μm. **E** shows that luciferase activity circRNA_0001103 after transfected with circ_0001103 WT, circ_0001103 Mut, miR-7240-5p mimic, or miR-7240-5p NC. The result shows that the luciferase activity of circRNA_0001103 is significantly decreased in circRNA_0001103 WT and miR-7240-5p mimic transfection group. **F** shows that luciferase activity SLC9A after transfected with SLC9A WT, SLC9A Mut, miR-7240-5p mimic, or miR-7240-5p NC. The result shows that the luciferase activity of SLC9A is significantly decreased in SLC9A WT and miR-7240-5p mimic transfection group. Data are presented as mean + SEM, n = 6 for each time point. **p < 0.001

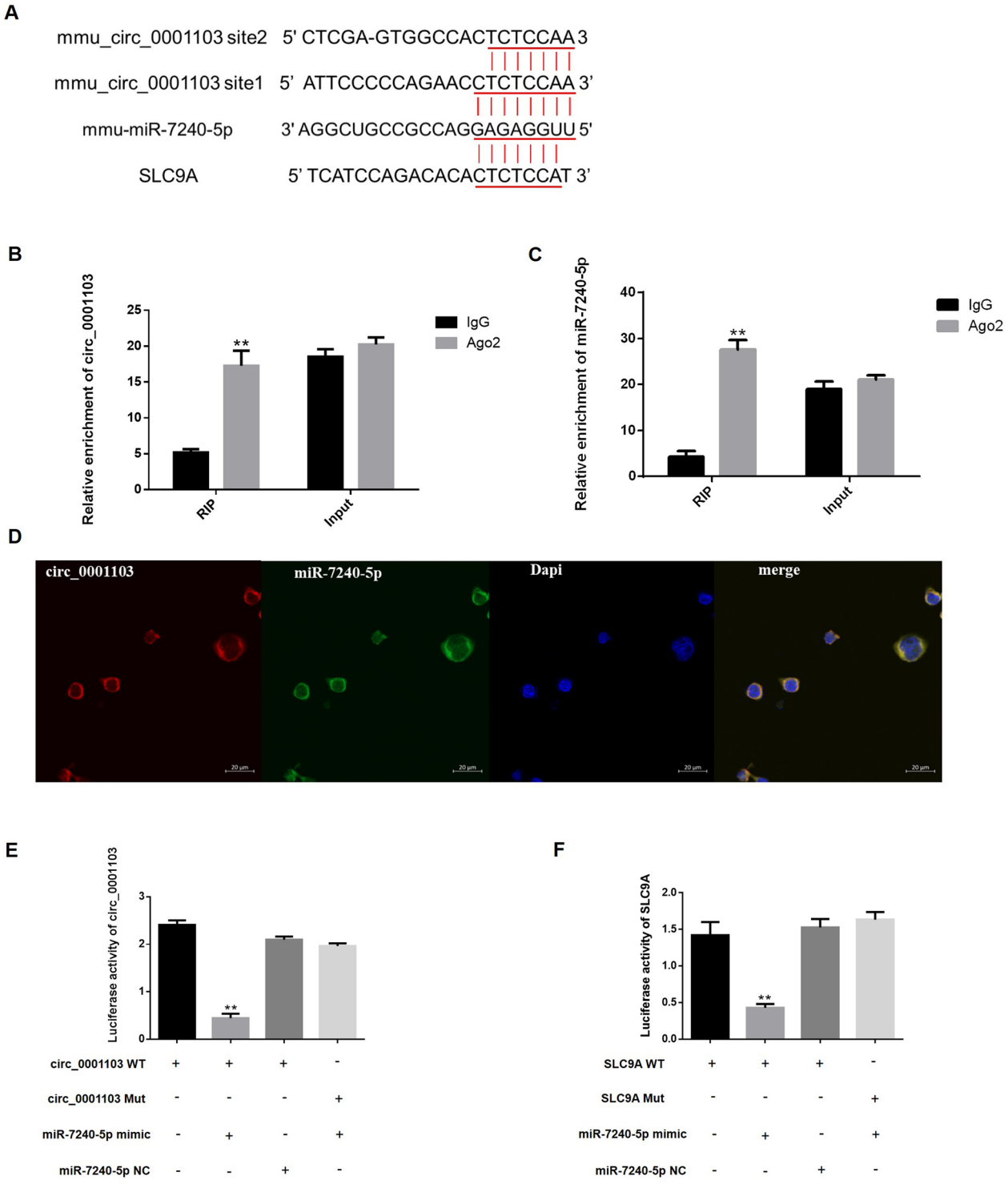

Fig. 5 (See legend on previous page.)

with macrophages F4/80 marker by paraffin sections and choroidal flatmounts, The formation of subretinal fibrosis can be influenced by intervention of MMT. Such, our results suggest that infiltrating macrophages may participate in macular fibrosis by transforming themselves into myofibroblasts.

TGF-β is a profibrotic mediator that can induce a variety of interstitial transformations including macrophage,

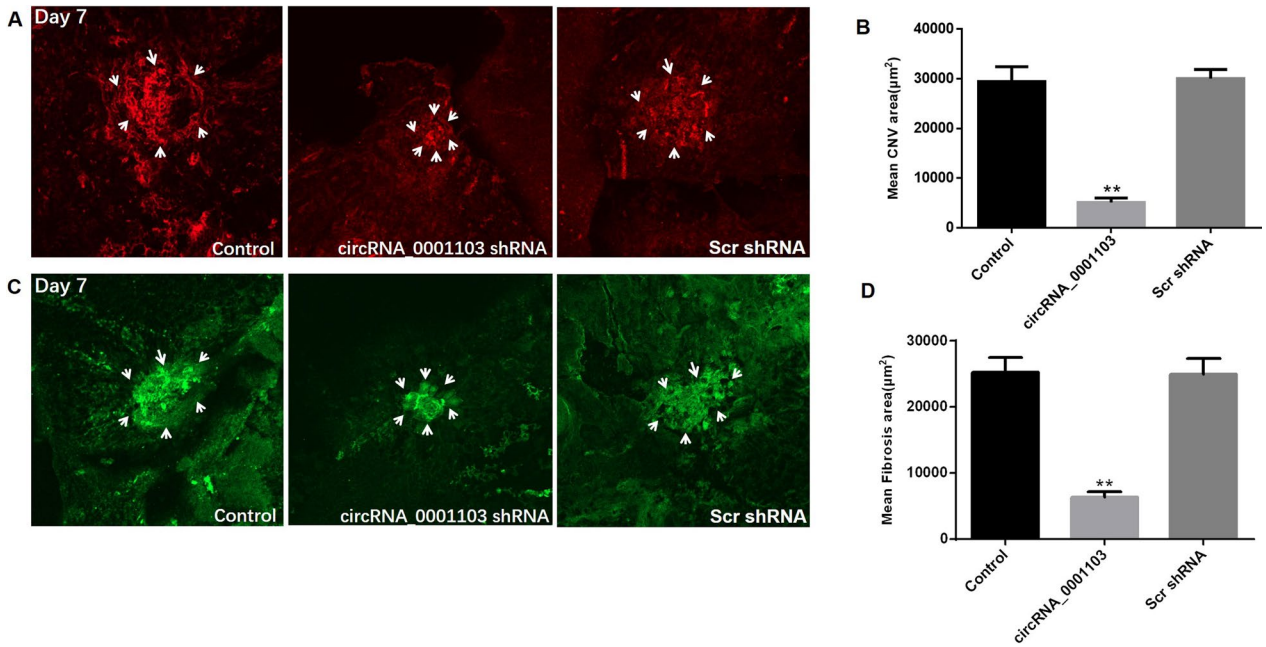

Fig. 6 Effects of circRNA_0001103 shRNA on CNV and subretinal fibrosis area. **A** showes choroidal flatmounts stained with isolectin B4 (CNV) at day 7. **B** showes the CNV area receiving circRNA_0001103 shRNA significantly reduced at day 7 ($p < 0.001$). **C** showes choroidal flatmounts stained with collagen I (fibrosis) at day 7. **D** showes the subretinal fibrosis area receiving circRNA_0001103 shRNAsignificantly reduced at day 7 ($p < 0.001$). All samples were received Intravitreal administration of circRNA_0001103shRNA or Scr shRNA at day 1 after laser induction of CNV. Data are presented as mean+SEM, n = 6 for each timepoint. $^{**}p < 0.001$

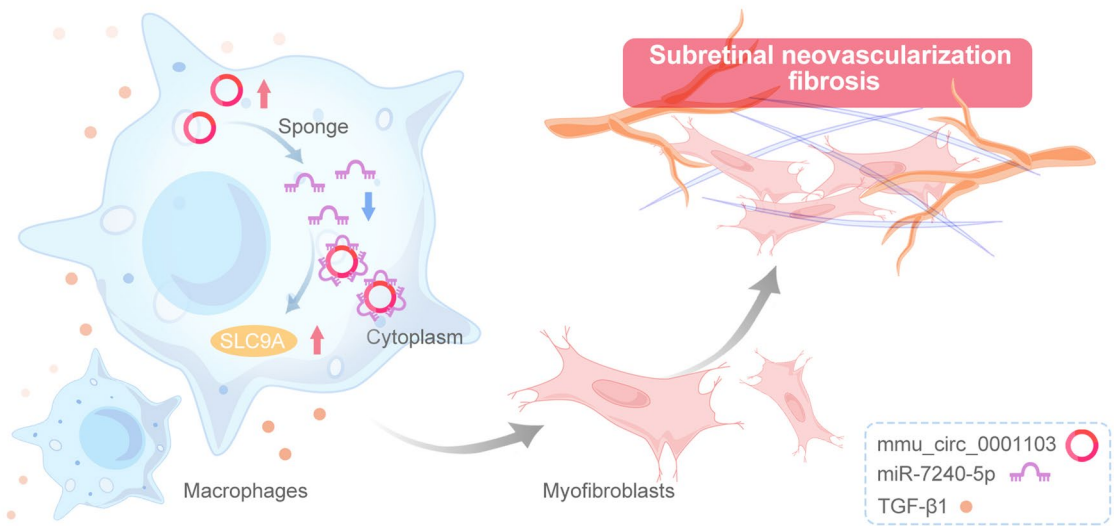

Fig. 7 Model of circRNA_0001103 function and the mechanism of regulation of macrophage to myofibroblast transition and subretinal fibrosis. The figure showed that circ_0001103 sponge adsorption miR-7240-5p regulates SLC9A1-mediated macrophage to myofibroblast transition and subretinal fibrosis and neovascularization. TGF-β1 is a major stimulator in macrophage to myofibroblast transition

PRE and endothelial cells [6]. Xu et al. have discovered that TGF-β1 was increased in the retina after laser treatment in CNV and subretinal fibrosis Mice model. Thus, in this study, we have used TGF-β1(2.5 ng/ml, 48 h) to stimulate raw264.7 macrophages to myofibroblasts transition. We detected α-SMA, a marker of MMT, and found that α-SMA expression were significantly increased at both mRNA and protein levels. These results have suggested that macrophages transform to myofibroblasts (MMT) during subretinal fibrosis and which is

involved in the formation of subretinal fibrosis. TGF-β1 may be a key driver of MMT in subretinal fibrosis.

CircRNAs are non-coding RNAs that are involved in regulating physiological and pathological responses within cells in a variety of ways [31]. CircRNAs' biological function is related to its localization in the cell. In the nucleus, circRNAs can activate genes transcription, or competitively bind to target genes, mediating genes expression. A better understanding of the impact of genetic inheritance is essential to advance personalized treatment approaches [32]. In the cytoplasm, circRNAs containing miRNA response elements (MREs) which can sponge adsorb downstream miRNAs or competitively bind to corresponding miRNA-binding sites to regulate the expression of target genes [33, 34].

Through sequencing screening, we found that circ_0001103 was expressed in both the laser-induced CNV and subretinal fibrosis mouse model and TGF-β1 induced MMT model. Through nucleoplasmic isolation and FISH experiments, it was found that circRNA_0001103 was mainly located in the cytoplasm. Bioanalysis showed that circRNA_0001103 had a binding site for miRNA-7240-5p. The results suggested that the molecular mechanism of circRNA_0001103 regulating MMT may be competitive binding of miRNA-7240-5p. Next, we used co-immunoprecipitation and dual luciferase assay. The results showed that compared with IgG group, there was an increasing trend in Ago2 group. The circ_0001103 wild-type + miR-7240-5p mimic group and SLC9A wild-type + miR-7240-5p mimic group of dual Luciferase were decreased. The combination of circRNA_0001103 with miRNA-7240-5p and miRNA-7240-5p with SLC9A was confirmed, that is, circRNA_0001103 regulates the expression of downstream target gene SLC9A through competitive binding with miRNA-7240-5p.

Finally, in order to verify the biological effects of mmu_circ_0001103, we used vitreous injection technology and found that after circ_0001103 was inhibited, both MMT and subretinal fibrosis were inhibited in mice, revealing that circ_0001103 is a potential molecular target to intervene in subretinal fibrosis.

In conclusion, in this study, we have found abnormal expression of circular RNA in the mouse model of CNV, further confirming that circ_0001103 may be a new target affecting subretinal fibrosis. Our results has implicated that macrophage to myofibroblast transition may be an important pathological process in the formation of subretinal fibrosis. Xu et al. found that macrophages undergo macrophage to myofibroblast transformation in a certain microenvironment, and these cells play an important role in the formation of subretinal fibrosis, which is consistent with our findings. Furthermore, we found that circ-0001103 can regulate the transformation of macrophages into myofibroblasts, affecting the formation of subretinal fibrosis, laying an experimental foundation for future intervention measures [18]. Although the studies have shown that circ_0001103 can sponge adsorption with miR-7240-5p, mediating macrophage to myofibroblast transition and subretinal fibrosis growth, there are still some limitations in this study. Firstly, whether circ_0001103 is expressed in human is unclear. There is a lack of experiments on humans in this study. Secondly, in this study, experiments were done in mice, and the number of animals was small. There was a lack of experiments and validation in larger sample sizes of mice and primates. Thirdly, the mechanism by which circ_0001103 regulates macrophage to myofibroblast transition and subretinal fibrosis is complex. In the future, more experiments are needed to be carried out in order to explore.

Supplementary Information

The online version contains supplementary material available at https://doi.org/10.1186/s12967-025-06173-3.

Supplementary Material 1: Figure S1. qRT-PCR tested the top 10 circRNAs of the microarray data of mice. The data showed that the expression of circ_0001103 was significantly higher than that of normal tissues on days 7, 14 and 28 after laser induction. circ_0000270, circ_0000273, circ_0000008, circ_0000214 were significantly higher than that of normal tissues on day 7 after laser induction, *p < 0.05, **p < 0.001.

Author contributions

Q.Z., B.L., L.H. and P.Z. designed and conduct of the study. Y.Z. and X.Z. analyzed data. K.F. and T.C. writed the manuscript. Y.L. and P.Z. revised the manuscript. All authors have read and approved the final manuscript.

Funding

This work was supported by the National Natural Science Foundation of China (Grant No. 81700867, 81901519), and the Talent Cultivation and International Academic Visiting Project for College Scholar of Anhui Province, China (Grant No. gxgwfx2019034).

Data availability

The original contributions presented in the study are included in the article; further inquiries can be directed to the corresponding author.

Declarations

Ethics approval and consent to participate

The study have been approved by the Animal Ethics Committee of Wannan Medical College (Approval No.2019-028) and follow ARRIVE guidelines. The animal study protocol was approved by the Animal Welfare Ethics Committee of Central South University.

Competing interests

The authors have no conflicts of interest to declare.

Author details

[1]Department of Ophthalmology, The First Affiliated Hospital of Wannan Medical College (Yijishan Hospital of Wannan Medical College), Wuhu 241001, Anhui, People's Republic of China. [2]Department of Ophthalmology, Huangshan People's Hospital, Huangshan 245200, Anhui, People's Republic of China. [3]Department of Ophthalmology, Yixing Eye Hospital, Yixing 214200, Jiangsu, People's Republic of China. [4]Department of Pathology, The First Affiliated

Hospital of Wannan Medical College (Yijishan Hospital of Wannan Medical College), Wuhu 241001, Anhui, People's Republic of China. [5]Central Laboratory, The First Affiliated Hospital of Wannan Medical College (Yijishan Hospital of Wannan Medical College), Wuhu 241001, Anhui, People's Republic of China.

Received: 11 October 2024 Accepted: 28 January 2025
Published online: 28 February 2025

References

1. Guymer RH, Campbell TG. Age-related macular degeneration. Lancet. 2023;401:1459–72.
2. Wang Y, Zhong Y, Zhang L, Wu Q, Tham Y, Rim TH, Kithinji DM, Wu J, Cheng C, Liang H, Yu H, Yang X, Liu L. Global incidence, progression, and risk factors of age-related macular degeneration and projection of disease statistics in 30 years: a modeling study. Gerontology. 2022;68:721–35.
3. Thomas CJ, Mirza RG, Gill MK. Age-related macular degeneration. Med Clin North Am. 2021;105:473–91.
4. Fleckenstein M, Keenan TDL, Guymer RH, Chakravarthy U, Schmitz-Valckenberg S, Klaver CC, Wong WT, Chew EY. Age-related macular degeneration. Nat Rev Dis Prim. 2021;7:31.
5. Song D, Liu P, Shang K, Ma Y. Application and mechanism of anti-VEGF drugs in age-related macular degeneration. Front Bioeng Biotechnol. 2022;10:943915.
6. Li X, Liu Y, Tang Y, Xia Z. Transformation of macrophages into myofibroblasts in fibrosis-related diseases: emerging biological concepts and potential mechanism. Front Immunol. 2024;15:1474688.
7. Liu D, Zhang C, Zhang J, Xu GT, Zhang J. Molecular pathogenesis of subretinal fibrosis in neovascular AMD focusing on epithelial-mesenchymal transformation of retinal pigment epithelium. Neurobiol Dis. 2023;185:106250.
8. Tenbrock L, Wolf J, Boneva S, Schlecht A, Agostini H, Wieghofer P, Schlunck G, Lange C. Subretinal fibrosis in neovascular age-related macular degeneration: current concepts, therapeutic avenues, and future perspectives. Cell Tissue Res. 2022;387:361–75.
9. Finn AP, Pistilli M, Tai V, Daniel E, Ying GS, Maguire MG, Grunwald JE, Martin DF, Jaffe GJ, Toth CA, Comparison of Age-Related Macular Degeneration Treatments Trials Research Group. Localized optical coherence tomography precursors of macular atrophy and fibrotic scar in the comparison of age-related macular degeneration treatments trials. Am J Ophthalmol. 2021;223:338–47.
10 ElSheikh RH, Chauhan MZ, Sallam AB. Current and novel therapeutic approaches for treatment of neovascular age-related macular degeneration. Biomolecules. 2022;12:1629.
11. Little K, Ma JH, Yang N, Chen M, Xu H. Myofibroblasts in macular fibrosis secondary to neovascular age-related macular degeneration - the potential sources and molecular cues for their recruitment and activation. EBioMedicine. 2018;38:283–91.
12. Little K, Llorian-Salvador M, Tang M, Du X, O'Shaughnessy O, McIlwaine G, Chen M, Xu H. A two-stage laser-induced mouse model of subretinal fibrosis secondary to choroidal neovascularization. Transl Vis Sci Technol. 2020;9:3.
13. Szczepan M, Llorian-Salvador M, Chen M, Xu H. Immune cells in subretinal wound healing and fibrosis. Front Cell Neurosci. 2022;16:916719.
14. Llorian-Salvador M, Byrne EM, Szczepan M, Little K, Chen M, Xu H. Complement activation contributes to subretinal fibrosis through the induction of epithelial-to-mesenchymal transition (EMT) in retinal pigment epithelial cells. J Neuroinflamm. 2022;19:182.
15 Shu DY, Butcher E, Saint-Geniez M. EMT and EndMT: emerging roles in age-related macular degeneration. Int J Mol Sci. 2020;21:4271.
16. Saki N, Haybar H, Aghaei M. Subject: Motivation can be suppressed, but scientific ability cannot and should not be ignored. J Transl Med. 2023;21:520.
17. Zhang P, Wang H, Luo X, Liu H, Lu B, Li T, Yang S, Gu Q, Li B, Wang F, Sun X. MicroRNA-155 inhibits polarization of macrophages to M2-type and suppresses choroidal neovascularization. Inflammation. 2018;41:143–53.
18. Little K, Llorian-Salvador M, Tang M, Du X, Marry S, Chen M, Xu H. Macrophage to myofibroblast transition contributes to subretinal fibrosis secondary to neovascular age-related macular degeneration. J Neuroinflamm. 2020;17:355.
19. Chen LL. The expanding regulatory mechanisms and cellular functions of circular RNAs. Nat Rev Mol Cell Biol. 2020;21:475–90.
20. Wang T, Li S, Li XM, Li C, Wang F, Jiang Q. Targeting circular RNA-Glra2 alleviates retinal neurodegeneration induced by ocular hypertension. Aging. 2023;15:10705–31.
21 Zhang M, Du G, Xie L, Xu Y, Chen W. Circular RNA HMGCS1 sponges MIR4521 to aggravate type 2 diabetes-induced vascular endothelial dysfunction. Elife. 2024;13: RP97267.
22 Thamjamrassri P, Ariyachet C. Circular RNAs in cell cycle regulation of cancers. Int J Mol Sci. 2024;25:6094.
23. Wu J, Chen J, Hu J, Yao M, Zhang M, Wan X, Jia H, Wang F, Sun X. CircRNA Uxs1/miR-335-5p/PGF axis regulates choroidal neovascularization via the mTOR/p70 S6k pathway. Transl Res. 2023;256:41–55.
24. Cheong KX, Cheung CMG, Teo KYC. Review of fibrosis in neovascular age-related macular degeneration. Am J Ophthalmol. 2023;246:192–222.
25. Aghaei M, Khademi R, Bahreiny SS, Saki N. The need to establish and recognize the field of clinical laboratory science (CLS) as an essential field in advancing clinical goals. Health Sci Rep. 2024;7: e70008.
26. Aghapour SA, Torabizadeh M, Bahreiny SS, Saki N, Jalali Far MA, Yousefi-Avarvand A, Dost Mohammad Ghasemi K, Aghaei M, Abolhasani MM, Sharifani MS, Sarbazjoda E, Javidan M. Investigating the dynamic interplay between cellular immunity and tumor cells in the fight against cancer an updated comprehensive review. Iran J Blood Cancer. 2024;16(2):84–101.
27. Yang X, Zou R, Dai X, Wu X, Yuan F, Feng Y. YAP is critical to inflammation, endothelial-mesenchymal transition and subretinal fibrosis in experimental choroidal neovascularization. Exp Cell Res. 2022;417:113221.
28. Zhang P, Lu B, Zhang Q, Xu F, Zhang R, Wang C, Liu Y, Wei C, Mei L. LncRNA NEAT1 Sponges MiRNA-148a-3p to suppress choroidal neovascularization and M2 macrophage polarization. Mol Immunol. 2020;127:212–22.
29 Boutilier AJ, Elsawa SF. Macrophage polarization states in the tumor microenvironment. Int J Mol Sci. 2021;22:6995.
30. Cutolo M, Campitiello R, Gotelli E, Soldano S. The role of M1/M2 macrophage polarization in rheumatoid arthritis synovitis. Front Immunol. 2022;13:867260.
31 Gu A, Jaijyan DK, Yang S, Zeng M, Pei S, Zhu H. Functions of circular RNA in human diseases and illnesses. Noncoding RNA. 2023;9:38.
32. Aghaei M, Khademi R, Far MAJ, Bahreiny SS, Mahdizade AH, Amirrajab N. Genetic variants of dectin-1 and their antifungal immunity impact in hematologic malignancies: a comprehensive systematic review. Curr Res Transl Med. 2024;72:103460.
33. Patop IL, Wust S, Kadener S. Past, present, and future of circRNAs. EMBO J. 2019;38: e100836.
34. Zhou WY, Cai ZR, Liu J, Wang DS, Ju HQ, Xu RH. Circular RNA: metabolism, functions and interactions with proteins. Mol Cancer. 2020;19:172.

Publisher's Note